Theoretical study of the addition and hydrogen abstraction reactions of the methyl radical with formaldehyde and hydroxymethylene

HUU THO NGUYEN[1]* and XUAN SANG NGUYEN[2]

[1]*Department of Natural Sciences Education, Saigon University, 273 An Duong Vuong St., District 5, Ho Chi Minh 700000, Vietnam and* [2]*Department of Electronics and Telecommunications, Saigon University, 273 An Duong Vuong St., District 5, Ho Chi Minh 700000, Vietnam*

Abstract: The mechanism, thermochemistry and kinetics of the addition and hydrogen-atom abstraction reactions of the methyl radical with formaldehyde and hydroxymethylene were investigated by *ab initio* calculations. The potential energy surface (PES) of the reactions were calculated by single point calculations at the CCSD(T)/6-311++G(3df,2p) level based on geometries at the B3LYP/6-311++G(3df,2p) level. The rate constants of various product channels were estimated by the variational transition state theory (VTST) and are discussed for the seven reactions in the temperature range of 300–2000 K and at 101325 Pa pressure. The calculated results showed that all the hydrogen abstraction reactions are more favorable than the addition ones.

Keywords: rate constants; hydrogen abstraction reactions; CCSD(T); B3LYP.

INTRODUCTION

Free radicals play a crucial role in chemical reactions. Most of the reactions in the fuel system, the earth's atmosphere and planets have involved free radicals. In fact, their mechanisms have been intensively studied recently.[1–4] The methyl radical CH_3, one of the most important free radicals due to its high reactive activity, is favored in combustion research. Recent results showed that it also participates in chemical vapor deposition (CVD) and chemical vapor infiltration (CVI) routes.[5–7] Among alkyl radicals, CH_3 shows an imperviable characteristic to thermal decomposition.[8] Formaldehyde $H_2C=O$, the first polyatomic organic compound observed in the interstellar medium and in dark nebulae, was predicted to be present in the Titan atmosphere. The $H_2C=O$ molecule is among the most abundant aldehyde molecules in the terrestrial lower atmosphere, where it is

---

* Corresponding author. E-mail: nguyenhuutho@sgu.edu.vn

1113

emitted, among other sources, from the combustion of fossil fuels and from biomass burning. In combustion systems, it lies on the primary oxidation pathway of natural gas and other alkane-based hydrocarbon fuels, *i.e.*, H_2CO emission from fuel engines increases with the use of oxygenated fuels, including methanol, ethanol, and methyl tertiary butyl ether blended fuels.[9] On the unimolecular rearrangement of formaldehyde, *ab initio* calculations proved that formaldehyde can isomerize to form *trans*- and *cis*-HCOH. However the isomerization barrier of ~78.87 kcal* mol^{-1} and a reaction endoergicity of ~47.80 kcal mol^{-1} means that the formation of these isomers are less favorable.[10] Hence, the study of the reactions CH_3 radicals with formaldehyde and alkanes is important to understand the process of hydrocarbon combustions. Many experimental and theoretical studies of the $CH_3 + CH_2O$ reaction system were performed[11–18] and the general consensus was that hydrogen abstraction is an important channel. Li *et al.* located stationary points on the $CH_3 + CH_2O$ potential energy surface at the QCISD(T)/ /6-311+G(3d*f*,2p)//MP2/6-311++G(d,p) levels of theory in a recent theoretical study.[15] However, their computed rate constant at 600 K was about two times slower than the recommended value which was based on the work of Choudhury *et al.*[16] By using a shock tube and modeling method, the reaction was studied over a large range of high temperatures. The modeling study was well fitted by quantum mechanical tunneling over the entire experimental range 300–1700 K. To the best of our knowledge, no work on the mechanism of the reaction of the methyl radical with hydroxymethylene has ever been performed, neither by experiment nor by theory. In this paper, we investigated the mechanism of the addition and hydrogen abstraction for reactions between formaldehyde and its isomers with methyl radical in the gas phase. The temperature dependence of rate constants from these reactions were verified and clarified.

COMPUTATIONAL DETAILS

All calculations were realized using the Gaussian 09 program.[19] Since the studied systems, methyl radical with formaldehyde and hydroxymethylene, are open-shell species, the density functional theory (DFT) method was superior in using the precise electron density to calculate the molecular characteristics. For calculations relating to open-shell systems using the DFT method, spin contamination does not affect the molecular properties.[20,21] The hybrid density functional method (B3LYP), Becke's three parameter nonlocal exchange functional[22-24] with the nonlocal correlation functional of Yang *et al.*[25] with 6-311++G(3df,2p) basis set[26] was used to optimize the geometries of the reactants, transition states (TS), and products. Frequencies calculations were performed at the same level to check whether the obtained stationary points are local minima or saddle points. Local minima and saddle points were confirmed to have all real frequencies and only one imaginary frequency, respectively. Then, vibrational frequencies of all species were scaled by a standard factor of 0.9679.[27] To achieve more reliable energies of various species, the CCSD(T)/6-311++G(3d,2p) method was employed to obtain the single point energy based on the optimized geometries.[28] Following the researches,
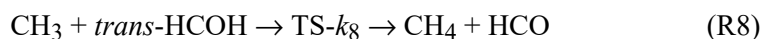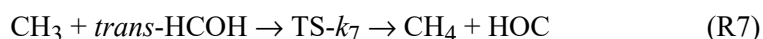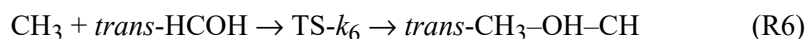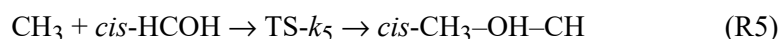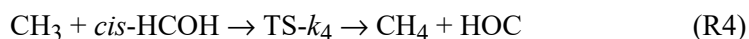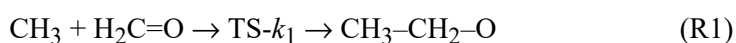
---

* 1 kcal = 4184 J

the use of calculated data from the CCSD(T)/B3LYP method with 6-311++G(3df,2p) basis set in estimating the rate constants of the gas phase reactions gave the good results.[29-33]

At 101325 Pa pressure, temperature dependent rate constants were collected using the variational transition state theory (VTST) with Eckart tunneling correction[34] and the KisThelp program.[35]

RESULTS AND DISCUSSION

In all systems, both addition and abstraction reaction paths were investigated:

$$CH_3 + H_2C=O \rightarrow TS\text{-}k_1 \rightarrow CH_3–CH_2–O \qquad (R1)$$

$$CH_3 + H_2C=O \rightarrow TS\text{-}k_2 \rightarrow CH_3–O–CH_2 \qquad (R2)$$

$$CH_3 + H_2C=O \rightarrow TS\text{-}k_3 \rightarrow CH_4 + HCO \qquad (R3)$$

$$CH_3 + cis\text{-}HCOH \rightarrow TS\text{-}k_4 \rightarrow CH_4 + HOC \qquad (R4)$$

$$CH_3 + cis\text{-}HCOH \rightarrow TS\text{-}k_5 \rightarrow cis\text{-}CH_3–OH–CH \qquad (R5)$$

$$CH_3 + trans\text{-}HCOH \rightarrow TS\text{-}k_6 \rightarrow trans\text{-}CH_3–OH–CH \qquad (R6)$$

$$CH_3 + trans\text{-}HCOH \rightarrow TS\text{-}k_7 \rightarrow CH_4 + HOC \qquad (R7)$$

$$CH_3 + trans\text{-}HCOH \rightarrow TS\text{-}k_8 \rightarrow CH_4 + HCO \qquad (R8)$$

Details of barrier heights and enthalpy changes of reactions are presented in the section *Barrier height and enthalpy changes of the reactions*, and the rate constants in the section *Rate constants*.

Barrier height and enthalpy changes of the reactions

Eight transition states were found in the reaction of methyl radicals with formaldehyde and hydroxymethylene. The geometries of the eight transitional structures are presented in Fig. 1. The potential energy surface (PES) is shown in Fig. 2 in which the energy of reactants ($CH_3 + H_2C=O$) was considered as zero energy. There were three transition states in the reaction of methyl radicals with formaldehyde, *i.e.*, addition to atom C of the molecule H_2CO *via* TS-k_1 (7.87 kcal mol^{-1}), addition to atom O *via* TS-k_2 (20.29 kcal mol^{-1}) and abstraction of atom H *via* TS-k_3 (9.89 kcal mol^{-1}). Thus, the barrier of the addition reaction to atomic C was slightly lower than that of the abstraction reaction and much lower than that of the addition to atomic O. These values are in good agreement with those from previous works by Che and Liu.[17,18]

For *trans*-HCOH molecules, three transitional structures were obtained, *i.e.*, TS-k_6 (86.94 kcal mol^{-1}) from the addition reaction, and TS-k_7 (58.70 kcal mol^{-1}) and TS-k_8 (50.95 kcal mol^{-1}) from abstraction reactions. The calculated values for the geometrical parameters of the compounds and a comparison to experimental references are presented in Table I. The geometrical parameters estimated from the B3LYP/6-311++G(3df,2p) method agree more with experimental values
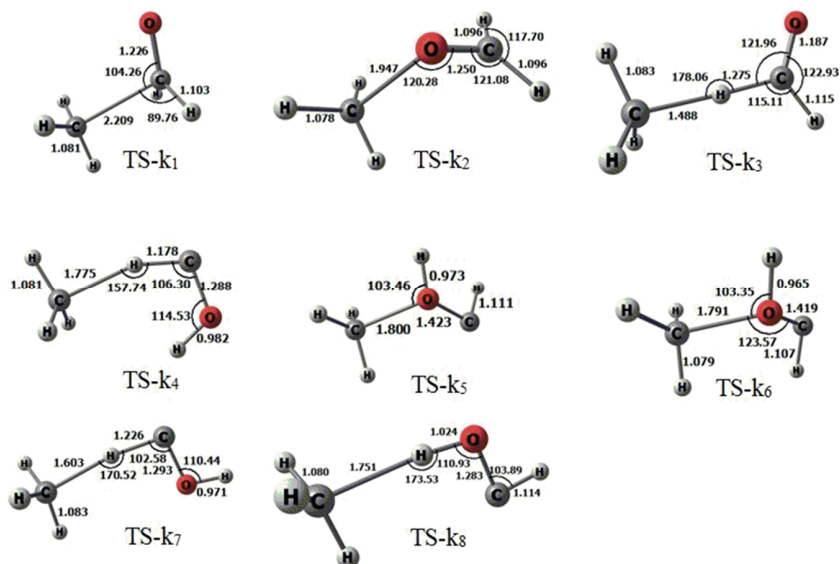
Fig. 1. Optimized geometries of the transition states obtained at the B3LYP/6-311++G(3df,2p) level of theory. Bond lengths are shown in Å, and angles are in degrees.
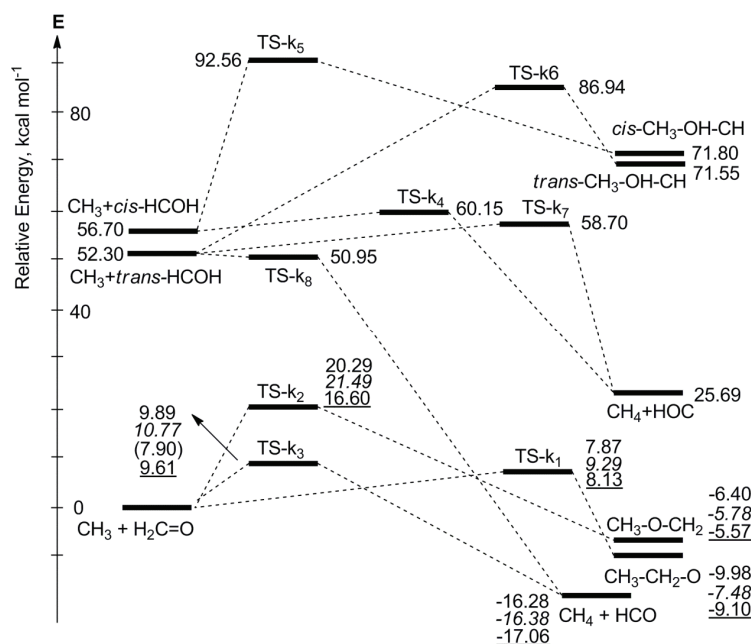
Fig. 2. Details of stationary points on PES (kcal mol⁻¹) of the $CH_3 + H_2CO$ and $CH_3 + HCOH$ reactions obtained at the CCSD(T)/B3LYP/6-311++G(3d,2p) level. The calculation values in italic[17] and underlined[18] were taken from theoretical papers. The value in parentheses was the experimental value from the literature.[36]

TABLE I. Geometrical parameters of the species

Species	Experimental	B3LYP/6-311++G(3df,2p)	MP2/6-311++G(3df,2p)
$H_2C=O$	d(C–H) = 1.111 Å	d(C–H) = 1.106 Å	d(C–H) = 1.101 Å
	d(C–O) = 1.205 Å	d(C–O) =1.199 Å	d(C–O) = 1.209 Å
	∠(HCH)=116.13°	∠(HCH)=116.08°	∠(HCH)=116.44°
	∠(HCO)=121.91°	∠(HCO)=121.96°	∠(HCO)=121.78°
	Ref. [37]		
CH_3	d(C–H) = 1.079 Å	d(C–H) = 1.078 Å	d (C–H) = 1.074 Å
	∠(HCH) = 120.00°	∠(HCH) = 120.00°	∠(HCH) = 120.00°
	Ref. [38]		
CH_4	d(C–H) = 1.0870 Å	d(C–H) = 1.0881 Å	d(C–H) = 1.0855 Å
	∠(HCH) = 109.471°	∠(HCH) = 109.471°	∠(HCH) = 109.471°
	Ref. [39,40]		

than those of the MP2/6-311++G(3df,2p) method.[37–40] Therefore, when using the database from the results of the CCSD(T)/B3LYP/6-311++G(3df,2p) method, a fault was found that the relative energy of TS-k_8 in R8 was lower by about 1.35 kcal mol^{−1} than that of reactants (CH_3 + *trans*-HCOH). Therefore the geometry of these structures in this reaction path were optimized at the MP2/6--311++G(3df,2p) level and the single point energy at CCSD(T)/6-311++G(3d,2p) level was calculated. As a result, the relative energy of TS-k_8 was slightly higher than that of the reactants (CH_3 + *trans*-HCOH) by 0.26 kcal mol^{−1}. After considering the results from both methods, it was confirmed that, in reality, the barrier height of this process was too low to distinguish them by the calculation methods.

For *cis*-HCOH molecules, only two transition states, *i.e.*, TS-k_4 (60.15 kcal mol^{−1}) of the H-abstraction reaction (R4) and TS-k_5 (92.56 kcal mol^{−1}) of the addition reaction (R5) were found. The calculation did not reveal a transition state for the abstraction reaction of H atom in the –CH group of the *cis*-HCOH molecule at the B3LYP/6-311++G(3d,2p) level, as opposed to the one for *trans*--HCOH *via* TS-k_8.

In the case of *trans*/*cis*-HCOH, all the barriers of the abstraction reactions were much lower than those of the addition reactions.

As shown in Table II, the enthalpy changes of the addition reactions of *cis*//*trans*-HCOH were positive and their reaction barriers were high and thus, the occurrence of these processes are unlikely. The enthalpy changes of the remaining reactions were negative, especially in the hydrogen-atom abstraction reactions of *cis*/*trans*-HCOH, which are very likely to occur. In the three reactions of formaldehyde, the barrier of the abstraction reaction was higher than that of the carbon-atom addition reaction. However, the enthalpy change of the abstraction reaction (–16.39 kcal mol^{−1}) was much lower than that of the carbon-atom addition reaction (–7.82 kcal mol^{−1}). This value is close that determined by Liu *et al.* (–16.53 kcal mol^{−1})[17] and the experimental value (–14.63 kcal mol^{−1}).[41]

TABLE II. Expression of the rate constant and enthalpy changes of reactions

Reaction	Rate constant, cm^3 mol^{-1} s^{-1}	ΔH^0_{298K} / kcal mol^{-1}	
		This study	from data[42]
(R1)	$k_1 = 4.394{\times}10^{-22}\ T^{2.76}\ \exp(-5.71\ \text{kcal mol}^{-1}/RT)$	−11.38	−11.71
(R2)	$k_2 = 4.137{\times}10^{-22}\ T^{2.90}\ \exp(-18.13\ \text{kcal mol}^{-1}/RT)$	−7.82	−8.74
(R3)	$k_3 = 2.644{\times}10^{-25}\ T^{4.22}\ \exp(-5.56\ \text{kcal mol}^{-1}/RT)$	−16.39	−16.69; −16.53[17]; −14.63[41] (Exp.)
(R4)	$k_4 = 1.064{\times}10^{-21}\ T^{3.08}\ \exp(-1.66\ \text{kcal mol}^{-1}/RT)$	−31.14	−31.03
(R5)	$k_5 = 7.136{\times}10^{-23}\ T^{2.91}\ \exp(-33.00\ \text{kcal mol}^{-1}/RT)$	13.97	
(R6)	$k_6 = 8.567{\times}10^{-23}\ T^{2.88}\ \exp(-31.82\ \text{kcal mol}^{-1}/RT)$	18.10	
(R7)	$k_7 = 1.174{\times}10^{-22}\ T^{3.58}\ \exp(-3.90\ \text{kcal mol}^{-1}/RT)$	−26.73	−26.62
(R8)	−	−68.71	−68.63

Rate constant

Resulting rate constant calculation values of (R3) are shown in Fig. 3 and Table III in the temperature range 300–2000 K. The obtained rate constant of (R3) agreed with experimental results,[16] and is better than the calculations in the work of Li *et al.*[15] At 600 K, the presented calculation showed that the rate constant of (R3) was $1.24{\times}10^{-15}$ cm^3 mol^{-1} s^{-1}, which is close to the experimental value ($1.20{\times}10^{-15}$ cm^3 mol^{-1} s^{-1}).[16]

Fig 3. Plot of the calculated rate constants, k_3 / cm^3 mol^{-1} s^{-1}, by the CCSD(T)/6-311++G(3d,2p) method and available experimental data *versus* 1000/T for (R3) at a pressure of 101325 Pa.

As mentioned above, the calculation for barrier height of TS-k_8 was faulty and hence, CCSD(T)/B3LYP/6-311++G(3df,2p) methods were not used to calculate the rate constant for the reaction *via* TS-k_8. The rate constants for seven reactions (R1)–(R7) are given in Table IV. These rate constant expressions were presented in Table II. These results have showed that rate constant of each abstraction reaction was higher than that of the addition one. Although the barrier of H-abstraction reaction of CH_3 with $H_2C{=}O$ was higher than that of C-addition of $H_2C{=}O$, the H-abstraction rate constant was higher. The rate constants of addi-

tion of *trans/cis*-HCOH molecules were quite small. These values are in agreement with the positive enthalpy changes of these reactions.

TABLE III. Rate constants for R3 and R1 in the temperature range 300–2000 K, at 101325 Pa pressure

| | k_3 / cm³ mol⁻¹ s⁻¹ | | | k_1/ cm³ mol⁻¹ s⁻¹ | | |
| | (CH₃ + H₂C=O → CH₄ + HCO) | | | (CH₃ + H₂C=O → CH₃–CH₂–O) | | |
T / K	This study	TST[15]	CVT/SCT[15]	Exp.[16]	This study	Review[43]	CVT/SCT[18]
300	$7.96{\times}10^{-19}$	$1.20{\times}10^{-19}$	$1.12{\times}10^{-18}$	$1.59{\times}10^{-17}$	$1.94{\times}10^{-19}$	$1.21{\times}10^{-17}$	–
400	$2.13{\times}10^{-17}$	$5.92{\times}10^{-18}$	$1.71{\times}10^{-17}$	$8.91{\times}10^{-17}$	$5.04{\times}10^{-18}$	$1.72{\times}10^{-16}$	$3.13{\times}10^{-17}$
600	$1.24{\times}10^{-15}$	$3.97{\times}10^{-16}$	$6.20{\times}10^{-16}$	$1.20{\times}10^{-15}$	$1.69{\times}10^{-16}$	$2.45{\times}10^{-15}$	$3.77{\times}10^{-16}$
800	$1.41{\times}10^{-14}$	$4.22{\times}10^{-15}$	$5.40{\times}10^{-15}$	$8.23{\times}10^{-15}$	$1.22{\times}10^{-15}$	$9.26{\times}10^{-15}$	$2.00{\times}10^{-15}$
1000	$7.44{\times}10^{-14}$	$2.07{\times}10^{-14}$	$2.41{\times}10^{-14}$	$3.80{\times}10^{-14}$	$4.54{\times}10^{-15}$	$2.05{\times}10^{-14}$	$6.99{\times}10^{-15}$
1200	$2.56{\times}10^{-13}$	$6.69{\times}10^{-14}$	$7.43{\times}10^{-14}$	$1.35{\times}10^{-13}$	$1.23{\times}10^{-14}$	$3.50{\times}10^{-14}$	$1.90{\times}10^{-14}$
1500	$1.02{\times}10^{-12}$	$2.49{\times}10^{-13}$	$2.66{\times}10^{-13}$	$6.51{\times}10^{-13}$	$3.61{\times}10^{-14}$	$5.95{\times}10^{-14}$	–
1600	$1.49{\times}10^{-12}$	$3.56{\times}10^{-13}$	$3.77{\times}10^{-13}$	$1.03{\times}10^{-12}$	$5.01{\times}10^{-14}$	$6.79{\times}10^{-14}$	–
1700	$2.11{\times}10^{-12}$	$4.95{\times}10^{-13}$	$5.20{\times}10^{-13}$	$1.58{\times}10^{-12}$	$6.42{\times}10^{-14}$	$7.64{\times}10^{-14}$	–
2000	$5.13{\times}10^{-12}$	$1.15{\times}10^{-12}$	$1.19{\times}10^{-12}$	$5.05{\times}10^{-12}$	$1.33{\times}10^{-13}$	$1.01{\times}10^{-13}$	–

TABLE IV. Rate constants, cm³ mol⁻¹ s⁻¹, for reactions R1–R7

T / K	k_1	k_2	k_3	k_4	k_5	k_6	k_7
300	$1.94{\times}10^{-19}$	$3.80{\times}10^{-28}$	$7.96{\times}10^{-19}$	$2.71{\times}10^{-15}$	$1.04{\times}10^{-39}$	$7.23{\times}10^{-39}$	$1.30{\times}10^{-16}$
400	$5.04{\times}10^{-18}$	$1.83{\times}10^{-24}$	$2.13{\times}10^{-17}$	$1.40{\times}10^{-14}$	$2.48{\times}10^{-33}$	$1.06{\times}10^{-32}$	$1.82{\times}10^{-15}$
500	$3.94{\times}10^{-17}$	$3.37{\times}10^{-22}$	$2.20{\times}10^{-16}$	$4.26{\times}10^{-14}$	$1.94{\times}10^{-29}$	$6.10{\times}10^{-29}$	$1.08{\times}10^{-14}$
600	$1.69{\times}10^{-16}$	$1.19{\times}10^{-20}$	$1.24{\times}10^{-15}$	$9.81{\times}10^{-14}$	$8.40{\times}10^{-27}$	$2.15{\times}10^{-26}$	$4.00{\times}10^{-14}$
700	$5.07{\times}10^{-16}$	$1.63{\times}10^{-19}$	$4.78{\times}10^{-15}$	$1.91{\times}10^{-13}$	$6.88{\times}10^{-25}$	$1.51{\times}10^{-24}$	$1.11{\times}10^{-13}$
800	$1.22{\times}10^{-15}$	$1.22{\times}10^{-18}$	$1.41{\times}10^{-14}$	$3.33{\times}10^{-13}$	$1.97{\times}10^{-23}$	$3.88{\times}10^{-23}$	$2.55{\times}10^{-13}$
900	$2.48{\times}10^{-15}$	$6.11{\times}10^{-18}$	$3.47{\times}10^{-14}$	$5.30{\times}10^{-13}$	$2.79{\times}10^{-22}$	$5.02{\times}10^{-22}$	$5.13{\times}10^{-13}$
1000	$4.54{\times}10^{-15}$	$2.28{\times}10^{-17}$	$7.44{\times}10^{-14}$	$8.14{\times}10^{-13}$	$2.40{\times}10^{-21}$	$4.03{\times}10^{-21}$	$9.33{\times}10^{-13}$
1100	$7.69{\times}10^{-15}$	$6.91{\times}10^{-17}$	$1.44{\times}10^{-13}$	$1.16{\times}10^{-12}$	$1.44{\times}10^{-20}$	$2.27{\times}10^{-20}$	$1.57{\times}10^{-12}$
1200	$1.23{\times}10^{-14}$	$1.78{\times}10^{-16}$	$2.56{\times}10^{-13}$	$1.61{\times}10^{-12}$	$6.51{\times}10^{-20}$	$9.84{\times}10^{-20}$	$2.49{\times}10^{-12}$
1300	$1.81{\times}10^{-14}$	$4.02{\times}10^{-16}$	$4.27{\times}10^{-13}$	$2.23{\times}10^{-12}$	$2.39{\times}10^{-19}$	$3.46{\times}10^{-19}$	$3.77{\times}10^{-12}$
1400	$2.64{\times}10^{-14}$	$8.29{\times}10^{-16}$	$6.76{\times}10^{-13}$	$2.89{\times}10^{-12}$	$7.39{\times}10^{-19}$	$1.03{\times}10^{-18}$	$5.46{\times}10^{-12}$
1500	$3.61{\times}10^{-14}$	$1.56{\times}10^{-15}$	$1.02{\times}10^{-12}$	$3.68{\times}10^{-12}$	$2.00{\times}10^{-18}$	$2.70{\times}10^{-18}$	$7.68{\times}10^{-12}$
1600	$5.01{\times}10^{-14}$	$2.75{\times}10^{-15}$	$1.49{\times}10^{-12}$	$4.62{\times}10^{-12}$	$4.82{\times}10^{-18}$	$6.35{\times}10^{-18}$	$1.05{\times}10^{-11}$
1700	$6.42{\times}10^{-14}$	$4.60{\times}10^{-15}$	$2.11{\times}10^{-12}$	$5.90{\times}10^{-12}$	$1.06{\times}10^{-17}$	$1.37{\times}10^{-17}$	$1.39{\times}10^{-11}$
1800	$8.47{\times}10^{-14}$	$7.39{\times}10^{-15}$	$2.90{\times}10^{-12}$	$7.40{\times}10^{-12}$	$2.16{\times}10^{-17}$	$2.73{\times}10^{-17}$	$1.82{\times}10^{-11}$
1900	$1.09{\times}10^{-13}$	$1.13{\times}10^{-14}$	$3.90{\times}10^{-12}$	$8.99{\times}10^{-12}$	$4.10{\times}10^{-17}$	$5.10{\times}10^{-17}$	$2.33{\times}10^{-11}$
2000	$1.33{\times}10^{-13}$	$1.64{\times}10^{-14}$	$5.13{\times}10^{-12}$	$1.06{\times}10^{-11}$	$7.39{\times}10^{-17}$	$9.00{\times}10^{-17}$	$2.93{\times}10^{-11}$

Figures 3 and 4, and Table III, show that the rate constants of (R1) and (R3) were in good agreement with experimental results at high temperatures. For example, at 2000 K, in cm³ mol⁻¹ s⁻¹ units, the calculations in this study were k_3 = = $5.13{\times}10^{-12}$ and $k_1 = 1.33{\times}10^{-13}$, in comparison to the experimental results of $k_3 = 5.05{\times}10^{-12}$ and $k_1 = 1.01{\times}10^{-13}$.

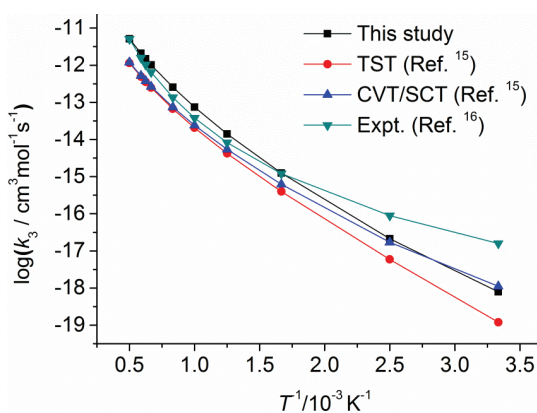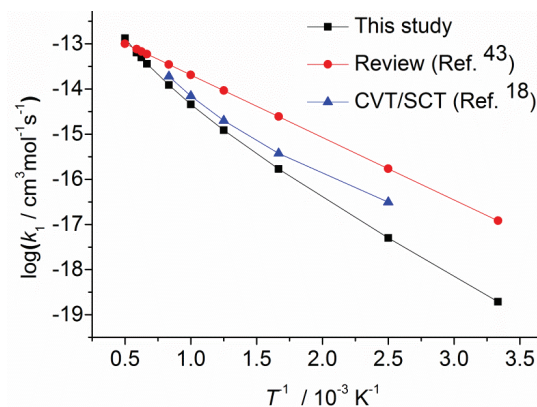Fig. 4. Plot of the calculated rate constants k_1 / cm^3 mol^{-1} s^{-1} in the CCSD(T)/6-311++G(3d,2p) method and available experimental data *vs.* 1000/*T* for (R1) at 101325 Pa pressure.

The temperature dependence of the branching ratios is illustrated in Fig. 5. In all temperature regions, the branching ratio of CH_3–O–CH_2 was negligibly small. At the highest temperature in this study, 2000 K, CH_3–O–CH_2 was 0.3 %. The pathway leading to product (CH_4+HCO) dominated over the entire studied temperature range. In the temperature range 300–2000 K, the branching ratio of CH_4+HCO increased gradually from 80.4 to 97.2 % while the branching ratio of CH_3–CH_2–O decreased gradually from 19.6 to 2.5 %.
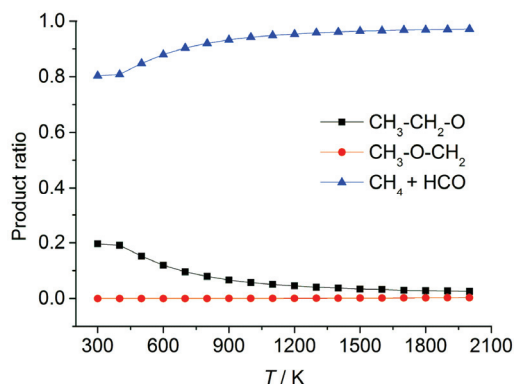

Fig. 5. The estimated branching ratios for the products for the CH_3 + H_2C=O reaction.

CONCLUSIONS

In this work, chemically accurate *ab initio* CCSD(T)/B3LYP/6--311++G(3df,2p) calculations of PES for the addition and hydrogen-atom abstraction reactions (CH_3 + H_2=CO) and (CH_3 + HCOH) were performed, followed by calculations of the rate constants by the VTST method. Enthalpy change values of reactions were estimated by the CCSD(T)/6-311++G(3d*f*,2p*)* method. The calculated results showed that the hydrogen abstraction reactions were the primary pathway in the temperature range from 300 to 2000 K. Three-parameter fittings of the calculated rate constants induced expressions for these reactions.

The rate constants of abstraction reactions for hydroxymethylene were much greater than those for formaldehyde. Moreover, the calculation results showed better agreement than previous works on rate constants of the addition and hydrogen abstraction reactions of the methyl radical with formaldehyde. This research may shed light on experimental studies and knowledge of the reaction mechanism of the methyl radical and hydroxymethylene.

И З В О Д

ТЕОРИЈСКО ИЗУЧАВАЊЕ АДИЦИЈЕ И АПСТРАКЦИЈЕ ВОДОНИКА У РЕАКЦИЈИ МЕТИЛ РАДИКАЛА СА ФОРМАЛДЕХИДОМ И ХИДРОКСИМЕТИЛЕНОМ

HUU THO NGUYEN[1] и XUAN SANG NGUYEN[2]

[1]*Department of Natural Sciences Education, Saigon University, 273 An Duong Vuong St., District 5, Ho Chi Minh 700000, Vietnam и* [2]*Department of Electronics and Telecommunications, Saigon University, 273 An Duong Vuong St., District 5, Ho Chi Minh 700000, Vietnam*

Механизам, термохемија и кинетика адиције и апстракције атома водоника код метил радикала у рекацији са формалдехидом и хидроксиметиленом истраживани су *ab initio* израчунавањима. Површине потенцијалне енергије (PES) реакција рачунате су *single point* израчунавањима на CCSD(T)/6-311++G(3df,2p) нивоу, на основу геометрија на B3LYP/6-311++G(3df,2p) нивоу. Константе брзина различитих канала ка производима процењене су и продискутоване за седам реакција у температурској области од 300–2000 K и на притиску од 101325 Pa, користећи варијациону теорију прелазног стања (VTST). Резултати израчунавања показују да су све реакције апстракције водоника много погодније од адиционих реакција.

(Примљено 4. јануара, ревидирано 20. марта, прихваћено 10. априла 2018)

REFERENCES

1. R. N. Hazlett, in *Frontiers of Free Radical Chemistry*, W. A. Pryor, Ed., Academic Press, Cambridge, MA, 1980, pp. 195–223
2. J. A. Kerr, in *Frontiers of Free Radical Chemistry*, W. A. Pryor, Ed., Academic Press, Cambridge, MA, 1980, pp. 171–193
3. A. Phaniendra, D. B. Jestadi, L. Periyasamy, *Indian J. Clin. Biochem.* **30** (2015) 11
4. V. Lobo, A. Patil, A. Phatak, N. Chandra, *Pharmacogn. Rev.* **4** (2010) 118
5. J. M. Simmie, H. J. Curran, *J. Phys. Chem. A* **113** (2009) 7834
6. L. Rutz, H. Bockhorn, J. W. Bozzelli, *Prepr. Symp. Am. Chem. Soc., Div. Fuel Chem.* **49** (2004) 451
7. S. L. Boyd, R. J. Boyd, *J. Phys. Chem. A* **105** (2001) 7096
8. I. R. Slagle, D. Sarzynski, D. Gutman, *J. Phys. Chem.* **91** (1987) 4375
9. H. M. T. Nguyen, H. T. Nguyen, T.-N. Nguyen, H. Van Hoang, L. Vereecken, *J. Phys. Chem. A* **118** (2014) 8861
10. G. F. Bauerfeldt, L. M. M. de Albuquerque, G. Arbilla, E. C. da Silva, *J. Mol. Struct.: THEOCHEM* **580** (2002) 147
11. T. K. Choudhury, W. A. Sanders, M. C. Lin, *J. Chem. Soc., Faraday Trans. 2* **85** (1989) 801
12. K. C. Manthorne, P. D. Pacey, *Can. J. Chem.* **56** (1978) 1307
13. C. Anastasi, *J. Chem. Soc., Faraday Trans. 1* **79** (1983) 749
14. H. Hippler, B. Viskolcz, *Phys. Chem. Chem. Phys.* **4** (2002) 4663
15. H.-Y. Li, M. Pu, Y.-Q. Ji, Z.-F. Xu, W.-L. Feng, *Chem. Phys.* **307** (2004) 35

16. T. K. Choudhury, W. A. Sanders, M. C. Lin, *J. Phys. Chem. A* **93** (1989) 5143
17. J.-y. Liu, Z.-s. Li, J.-y. Wu, Z.-g. Wei, G. Zhang, C.-c. Sun, *J. Chem. Phys.* **119** (2003) 7214
18. C.-b. Che, H. Zhang, X. Zhang, Y. Liu, B. Liu, *J. Phys. Chem. A* **107** (2003) 2929
19. *Gaussian 09, Revision C.01*, Gaussian, Inc., Wallingford CT, 2009
20. A. Hatipoglu, D. Vione, Y. Yalçın, C. Minero, Z. Çınar, *J. Photochem. Photobiol., A* **215** (2010) 59
21. B. Erem, G. Y. Y. Gurkan, *J. Serb. Chem. Soc.* **82** (2017) 277
22. A. D. Becke, *J. Chem. Phys.* **97** (1992) 9173
23. A. D. Becke, *J. Chem. Phys.* **96** (1992) 2155
24. A. D. Becke, *J. Chem. Phys.* **98** (1993) 5648
25. W. Yang, R. G. Parr, C. Lee, *Phys. Rev. A* **34** (1986) 4586
26. W. J. Hehre, L. Radom, P. v R. Schleyer, J. Pople, Ab Initio *Molecular Orbital Theory*, Wiley, New York, 1986, p. 79
27. M. P. Andersson, P. Uvdal, *J. Phys. Chem. A* **109** (2005) 2937
28. K. Raghavachari, G. W. Trucks, J. A. Pople, M. Head-Gordon, *Chem. Phys. Lett.* **157** (1989) 479
29. R. S. Zhu, K.-Y. Lai, M. C. Lin, *J. Phys. Chem. A* **116** (2012) 4466
30. R.-C. Jian, C. Tsai, L.-C. Hsu, H.-L. Chen, *J. Phys. Chem. A* **114** (2010) 4655
31. H.-J. Li, H.-L. Chen, J.-G. Chang, H.-T. Chen, S.-Y. Wu, S.-P. Ju, *J. Phys. Chem. A* **114** (2010) 5894
32. M.-K. Hsiao, Y.-H. Chung, Y.-M. Hung, H.-L. Chen, *J. Chem. Phys.* **140** (2014) 204316
33. H.-L. Chen, W.-C. Chao, *J. Phys. Chem. A* **115** (2011) 1133
34. M. Robson Wright, *Advances in Carbohydrate Chemistry*, Wiley, New York, 2005, p. 79
35. S. Canneaux, F. Bohr, E. Henon, *J. Comput. Chem.* **35** (2014) 82
36. J. A. Kerr, M. J. Parsonage, *Evaluated Kinetic Data on Gas Phase Hydrogen Transfer Reactions of Methyl Radicals*, Butterworths, London, 1976, p. 79.
37. L. V. Gurvich, I. V. Veyts, C. B. Alcock, *Thermodynamic Properties of Individual Substances*, Hemisphere Pub., New York, 1989
38. G. Herzberg, *Molecular Spectra and Molecular Structure*, *Vol. 3*, *Electronic spectra and electronic structure of polyatomic molecules*, Van Nostrand, New York, 1966
39. L. M. Sverdlov, M. A. Kovner, E. P. Krainov, *Vibrational Spectra of Polyatomic Molecules*, Wiley, New York, 1974
40. E. Hirota, *J. Mol. Spectrosc.* **77** (1979) 213
41. M. W. Chase, National Institute of Technology, *NIST-JANAF thermochemical tables*, American Chemical Society; American Institute of Physics for the National Institute of Standards and Technology, Washington, D.C.; Woodbury, N.Y., 1998, p. 79
42. http://garfield.chem.elte.hu/Burcat/burcat.html (October, 2017)
43. H. J. Curran, *Int. J. Chem. Kinet.* **38** (2006) 250.